crystals

Article

Quantitative Analysis of the Geometrically Representative Volume Element of the Yellow River's Granular Ice Microstructure during the Freezing Period

Yu Deng [1,2], Juan Wang [3,*], Jiao Zhou [3] and Peng Zhang [3]

1 Yellow River Institute of Hydraulic Research, Zhengzhou 450003, China; lanson0201@aliyun.com
2 Research Center on Levee Safety Disaster Prevention, MWR, Zhengzhou 450003, China
3 Yellow River Laboratory, Zhengzhou University, Zhengzhou 450001, China; zzuzhoujiao@163.com (J.Z.); zhangpeng@zzu.edu.cn (P.Z.)
* Correspondence: wangjuan@zzu.edu.cn

Abstract: As a naturally polycrystalline material, Yellow River ice exhibits complex mechanical properties that are closely related to its internal microstructure. To study the micromechanical properties of this ice, the geometrically representative volume element (RVE) and a method for determining it are proposed. By observing and quantifying trends in the microstructural characteristics of the granular ice, a micro-numerical model of Yellow River ice is established. Based on the calculations and analyses of randomness and similarity across model samples, the dimensions of a geometric RVE of granular ice in the Yellow River are quantitatively determined. The research shows that the geometric representation of Yellow River granular ice is 20–24 times larger than the average grain of Yellow River granular ice. These results provide a technique to accurately study, at a microscopic level, the relationship between the material properties of each phase and their macromechanical response. It also provides a theoretical basis for studying the fracture failure mechanism of Yellow River ice at multiple scales.

Keywords: ice; RVE; microstructure; Yellow River

Citation: Deng, Y.; Wang, J.; Zhou, J.; Zhang, P. Quantitative Analysis of the Geometrically Representative Volume Element of the Yellow River's Granular Ice Microstructure during the Freezing Period. *Crystals* **2023**, *13*, 1021. https://doi.org/10.3390/cryst13071021

Academic Editor: Borislav Angelov

Received: 9 May 2023
Revised: 18 June 2023
Accepted: 26 June 2023
Published: 28 June 2023

1. Introduction

River ice is a composite material with microscopic components that contain all of the structural properties of ice, such as the type, density, bubbles, and impurities [1]. Due to the different geographical environments, hydrometeorology, and other conditions of ice, the micro-components of ice also demonstrate differences [2]. The macroscopic properties of river ice are a reflection of its microstructural changes. These changes affect the macroscopic properties of the ice, such as temperature and density, which also affect the mechanical fracture properties [3]. Therefore, the fracture mechanism of river ice cannot be fully understood from the macroscopic view. It is thus necessary to quantify a representative volume element (RVE) of river ice's microstructure to provide a basis and reference for the analysis of the fracture process of the macroscopic ice cover. For an RVE of ice to effectively capture the underlying physics, it must represent not only the microstructure but also the material and performance of the river ice; therein, the macro- and microstudy of ice's material fracture performance in the Yellow River can be reconciled.

The concept of RVE was first proposed by Hill [4] in 1963 and then continuously improved by Hashin [5], Trusov [6], Ostoja-Starzewsk [7], Trias [8], and others. RVE has been applied to the study of ceramics [9], soil [10,11], metals [12], concrete [13], polymers [14], and other materials, but there are few reports on the research of an RVE of ice. As reported previously, there are three main methods to determine an RVE: The first is an analytical method based on the effective modulus, which obtains the smallest representative size (approximately 2–3 times the characteristic size). For example, Drugan [15] used a nonlocal constitutive equation to determine the representative size of the effective modulus of composite materials. The representative size was approximately twice the particle size of the reinforcement phase. Kerner [16] proposed a generalized self-consistent model, which was improved by Christensen and Lo [17] in 1979 and extended to the case of multiple inclusions by Herve and Zaoui [18] in 1993. Pensee et al. [19] found that the representative size was within three times the characteristic size. The second method is a numerical method based on the equivalent modulus [20,21], which obtains a representative size that is relatively dispersed due to size-dependent changes in the material properties (ranging from 5 to 50 times the characteristic scale) [22,23]. Previous reports [24–26] show different results for different representative materials. Compared to those reports, Kanit [27] derived the size of the representative voxel satisfying statistical uniformity and the number of numerical realization samples with a certain accuracy. The third method is an observation-based method including graphical analysis. Romero and Masad [28] studied the representative size of asphalt concrete by combining image analysis technology and test results. Graham and Yang [29] studied the distribution characteristics of the second phase in the alloy with an image analysis method. Al Raoush [30] studied the representative volume elements of natural sand samples through X-ray photography technology.

These reports show that methods of determining a representative body can be divided according to the determination strategy. Because the microstructure of river ice is complex, it is difficult to derive an analytical expression for its strength, while experimental observation makes it difficult to match the microstructure with the results of macromechanical tests. Thus, we deem numerical simulation to be the most effective approach. This study focuses on the microstructural characteristics of Yellow River ice. A micro-numerical model of Yellow River ice is constructed, and the geometric representative size of the microstructure of Yellow River ice is quantitatively analyzed based on the definition of geometric representation.

The research results in this paper bridge mesoscale and macroscopic research on river ice and provide methodological support for studying the macroscopic mechanical properties of river ice. The strength-based RVE of river ice can be determined based on the established geometric RVE of river ice to realize the transition from microscopic to macroscopic. Then, through homogenization, the geometric RVE of river ice can be used to generate a macroscopic model of river ice, which provides support for in-depth analysis of the fracture and failure of river ice.

2. Geometric Characteristics of Yellow River Ice's Microstructure

Due to the complexity of geography and climate, ice exhibits different formation processes in different regions, affecting the crystal types and the distribution of impurities in the ice. To study the microscopic structure of the Yellow River ice, ice samples in typical river sections were selected during the freezing period to observe their microstructures, including the type and size of ice crystals and the sediment and bubble contents.

2.1. Observation of the Ice Microstructure of the Yellow River

The differences in the microstructural characteristics of Yellow River ice depend on the thermal and hydraulic conditions of the Yellow River ice's growth. The annual average freezing period of the Yellow River is from early December to late March of the following year. Considering the local temperature changes, ice samples were taken in February. For many years, in Inner Mongolia, the Toudaoguai River section of the Yellow River has often been the first section to freeze. The Yellow River's central station for ice monitoring is located there, and it is also the section where ice samples were collected for this study. The Toudaoguai River Station is located at 111°04′ E and 40°16′ N. A map of the river section is shown in Figure 1. The frozen scene of the Toudaoguai Hydrological Station and the collected ice sample are shown in Figure 2. Due to the influence of upstream reservoir regulation, the river discharge varied between 200 m^3/s and 400 m^3/s during the initial freezing period and between 600 m^3/s and 800 m^3/s during the stable freezing period. The peak river discharge can reach 1000 m^3/s in the ice break-up period.

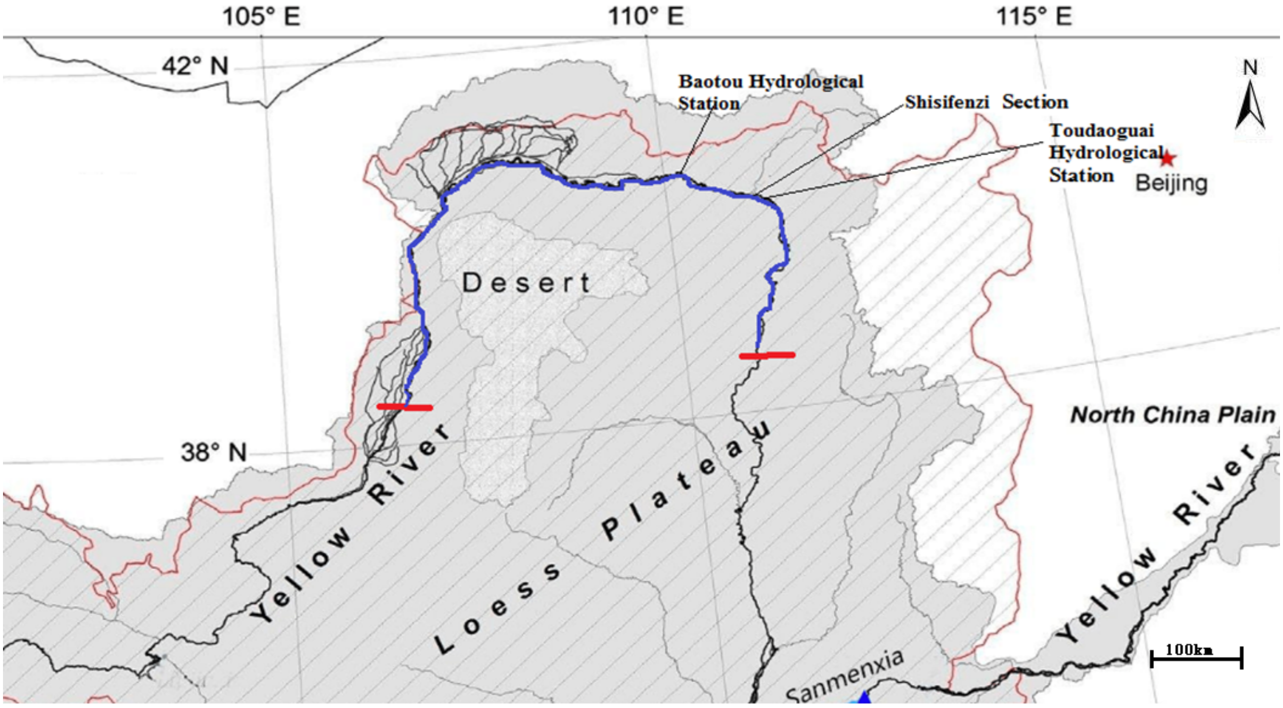

Figure 1. Schematic diagram of ice sample collection in the Yellow River.

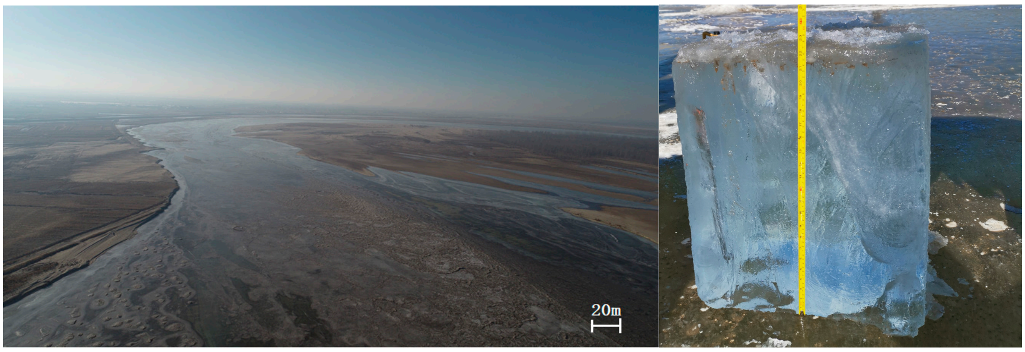

(**a**) (**b**)

Figure 2. Frozen scene of the Toudaoguai Hydrological Station section of the Inner Mongolia reaches of the Yellow River: (**a**) Toudaoguai Hydrological Station section; (**b**) ice sample collected from the Toudaoguai Hydrological Station section.

2.2. Experimental Design

To ensure the representativeness of the collected river ice, 13 samples were collected at different locations using electric drills, electric saws, steel rulers, and other tools. The samples were transported to a low-temperature laboratory. The specific sample collection method and principle can be found in reference [31]. In a low-temperature test room, the ice samples were cut every 8 cm from the direction perpendicular to the spindle and were processed into ice sheets with a thickness of less than 1 mm by manual grinding. Horizontal crystal sheets and vertical crystal sheets were obtained. The ice sheet samples for the ice microstructure test are shown in Figure 3.

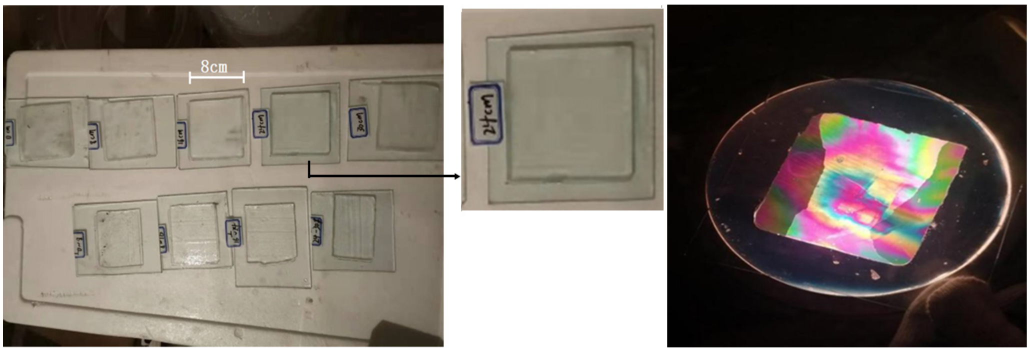

(**a**) (**b**)

Figure 3. Representative ice sheet samples: (**a**) ice sheets in natural light; (**b**) ice sheet in polarized light.

The universal stage was the primary piece of equipment for observation and testing. In a dark, opaque environment below −5 °C, the position of the polarizer was adjusted, river ice crystal flakes were placed sequentially on the observation platform, the ice crystals were imaged under an orthogonal polarizer, and the crystal type and crystal size were determined. The crystal types were mainly divided into granular ice and columnar ice. The crystal size is discussed in detail in Section 2.4.1. Then, images were recorded without an orthogonal polarizer to determine the distribution and size of the bubbles in the ice. The scale of both crystal and bubble pictures was 10 cm. The ice microstructure map obtained from the experiment was imported into MATLAB, and the built-in digital image package was used for preprocessing. Then, the Canny algorithm was used to extract and record the microscopic unit scale of the ice. This algorithm is an edge detection algorithm that has strong resistance to noise and can effectively extract the boundaries of ice crystal images [32]. The sediment content in the ice was mainly calculated by calculating the ratio of the sediment mass after drying to the ice mass before drying.

2.3. Ice Grain Image Processing

The following is an example of the ice grain image process of extracting ice grain boundaries based on the MATLAB digital image processing method. The original ice images are shown in Figure 4a, and there exist a large number of non-grain parts in the images. To facilitate subsequent digital image processing, the maximum inscribed rectangle of the ice images was divided based on the original images, and the actual length corresponding to the images was recorded to facilitate subsequent image conversion. Due to the complex computation and operation of color images during image processing, the images were converted into grayscale after recording, as shown in Figure 4b. At this time, there remained some noise in the ice images, which affected the results of boundary extraction. Therefore, the median filtering method was selected for noise reduction processing of the ice grain images. The median filtering method is a nonlinear digital filter technique, which is often used to remove noise from images or other signals. The design idea is to check the sampling in the input signal and determine whether it represents the signal; this function is achieved with an observation window composed of odd sampling [33]. When performing filtering and removing noise, it is necessary to select an appropriate neighborhood. If the selected neighborhood is relatively small, some large-area noise cannot be removed. If the selected neighborhood is too large, it leads to image distortion and obscure grain boundaries. Finally, a neighborhood of 24 pixels was selected for filtering, as shown in Figure 4c.

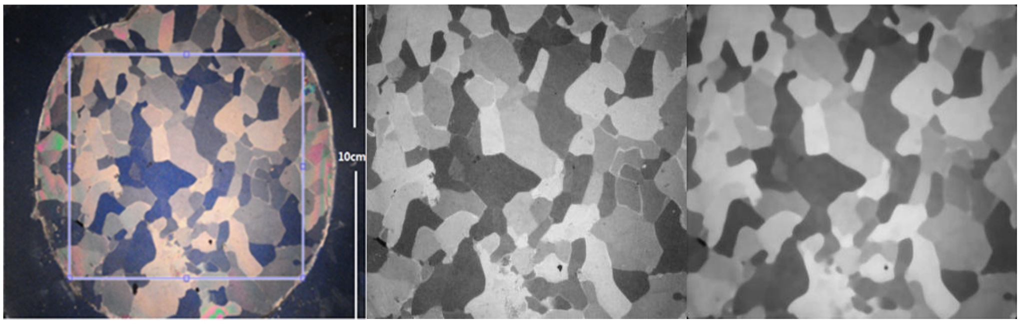

(**a**) (**b**) (**c**)

Figure 4. Image processing of ice grains: (**a**) Original ice image. (**b**) Gray transformation of ice grains. (**c**) Median filtering process.

After the ice grain image preprocessing was completed, the Canny operator was used to extract the boundaries of the ice images. When the images are segmented, it is necessary to select appropriate parameters to minimize the phenomenon of redundant and missing boundaries. If the extracted boundary image still contains missing or redundant boundaries, it is necessary to further correct the boundary images. First, discontinuous boundaries were automatically connected and processed. The boundary images are black and white images, and the broken boundary edge pixel points exist in nine pixel points centered on the boundary pixel points. Only one direction of the pixel is the same as the edge pixel, and all pixel points in other directions are black. By observing the characteristics, broken boundary points in the images can be detected and detection can be performed within a range of 7×7 pixels around the boundary point. In this case, if there exist other boundary points, they are connected with those already considered. After connecting the redundant boundaries, they were removed using Photoshop software. Then, the connected regions were assigned different gray values with MATLAB. The number of pixel points corresponding to each gray value was used as the pixel area of the ice grain, and the number of pixel points connecting the boundary region was used as the pixel perimeter of the ice grain.

2.4. Analysis of Observation Results

2.4.1. Ice Crystal Size Distribution

When observing the horizontal and vertical sections of river ice, the average density of ice in the Yellow River ranged from 0.77 g/cm^3 to 0.99 g/cm^3. The ice crystal types were identified and mainly divided into granular and columnar ice. This study focuses on the analysis of granular ice of the Yellow River, and the size distribution of ice crystals is analyzed according to two working conditions: the direction parallel to the C-axis (i.e., the ice crystal growth direction), and the direction perpendicular to the C-axis. In the direction parallel to the C-axis, the crystal structure of the cross-section of granular ice changed little; the distribution of the equivalent diameter (i.e., the diameter of ice crystals described by the equivalent circle diameter equal to the ice crystal area) of ice grains in the direction perpendicular to the C-axis is shown in Figure 5. In the vertical C-axis direction, the equivalent diameter of granular ice varied from 0.05 mm to 15 mm, and different ice grain sizes exhibited different proportions within a single sample. Many ice grains had an equivalent diameter of 2–3 mm—specifically, 25.4% of the grains. At diameters greater than 3 mm, the number of ice grains decreased with increasing equivalent diameter. There were few ice grains with large particles of granular ice: the proportion of ice grains with equivalent diameters greater than 10 mm was only 2.4% of the total count.

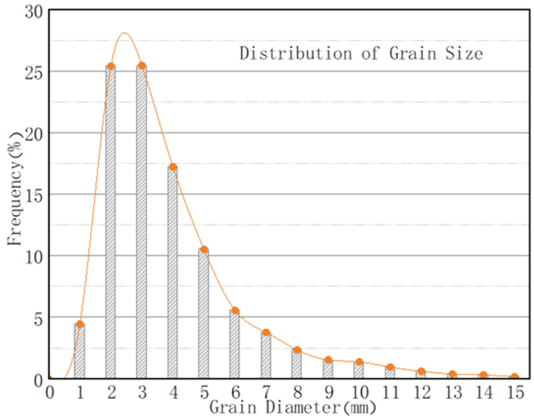

Figure 5. Distribution of ice particle size in the Yellow River.

2.4.2. Bubble Distribution

As a common impurity in river ice, bubbles significantly influence the physical properties and fracture mechanics of river ice. The bubble shape in Yellow River ice is shown in Figure 6, which shows that the bubbles in the granular ice are mainly spherical. Using the same processing method as for the ice crystal images, images of bubbles were processed in natural light; the statistical results of bubbles' content and equivalent diameter in the ice are shown in Figure 7, which shows that the equivalent diameter of bubbles in ice remains constant at approximately 0.225 mm with increasing depth. However, there is a clear change in the bubble content at different depths.

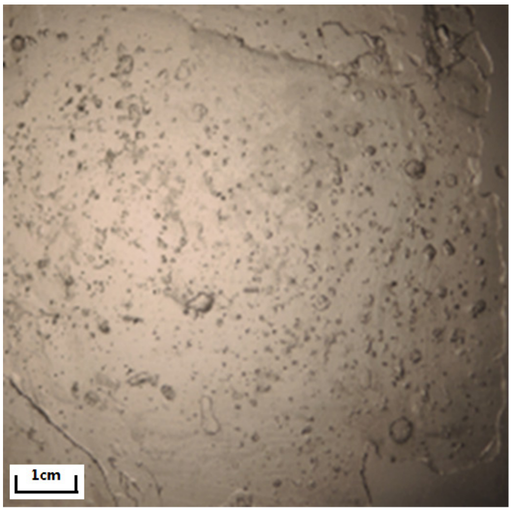

Figure 6. Bubbles' shape in Yellow River ice.

On the surface, the bubble content increases to 8.5% of the volume. With the growth of the ice layer, the bubble content gradually decreases, and the minimum content is only 1%. According to the analysis of the hydraulic change characteristics of the Yellow River, there are many bubbles on the surface, mainly because the water surface is subject to wind, waves, and other phenomena, resulting in a large amount of air being drawn into the water body that cannot be discharged before the temperature suddenly drops and the water freezes. However, with increasing depth, the bubbles in the ice mainly originate from trace gases that are not removed from the water.

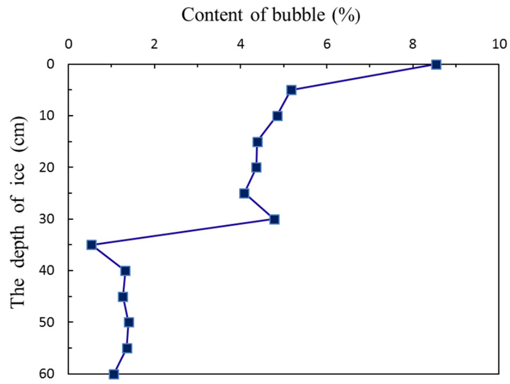

(**a**)

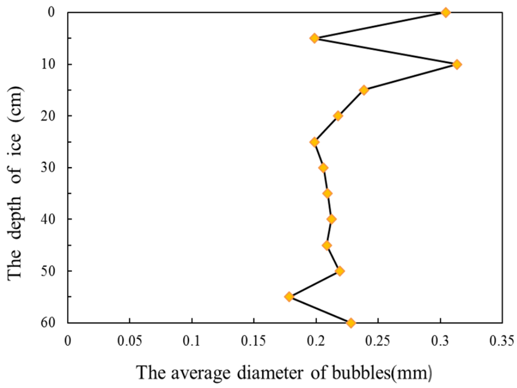

(**b**)

Figure 7. Bubbles' distribution in Yellow River ice: (**a**) the bubble content varies with the growth of the ice layer; (**b**) the average diameter of bubbles varies with the growth of the ice layer.

2.4.3. Sediment Distribution

Due to the special basin characteristics of the Yellow River, much sediment is carried in the river, resulting in Yellow River ice containing not only bubbles but also sediment impurities. In fact, this is a typical characteristic of Yellow River ice. To analyze the influence of sediment content in Yellow River ice, the sediment content in the river ice at different locations was measured with specific gravity in a drying oven. At first, the ice samples were melted, filtered, and dried, and then the weight of the dry sediment was measured, so that the sediment content per unit volume of the ice sample could be calculated. Figure 8 shows that the sediment content in the river ice gradually decreases with increasing depth, but the sediment content in different ice layers changes little and fluctuates around 0.5 kg/m^3.

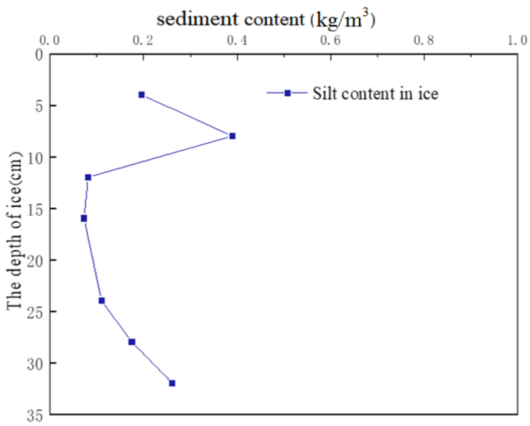

Figure 8. Variation in the ice and sediment contents of the Yellow River.

3. Microscopic Numerical Model of Yellow River Ice

3.1. Model Building Method

Due to the random shapes of river ice crystals, the Tyson polygon method (Voronoi algorithm) was used to randomly construct ice crystals and to simulate the crystal structure of river ice. This method constructs continuous polygons comprising perpendicular bisectors connecting two adjacent point segments. The distance from any point to the control points is less than the distance from other polygon control points within a Tyson polygon [34]. The Voronoi algorithm is widely used in the analysis of rock, metals, foam, and other materials due to its special mode of data processing. In the river ice model, the Voronoi polygon more closely resembles actual ice crystals; that is, the Voronoi algorithm can intuitively reveal the complex microgeometric information in river ice.

To match the size and contents of the ice crystal model to observations, and to ensure the random distribution of the size and coordinate position of the river ice microstructure, the corresponding particle flow is generated through the particle flow code (PFC) based on river ice observations. Thus, the area occupied by polygons with different equivalent particle sizes in the Voronoi diagram is controlled while the coordinates of the particle centers are calculated.

The PFC studies the mechanical properties and material behaviors from the microscopic perspective. The particles in the PFC are rigid, but overlapping mechanical relationships are allowed to simulate the contact force between particles. The mechanical relationship between particles adopts Newton's second law, and the contact failure between particles can take the form of shear and opening. The main fields of PFC application include civil engineering, mining engineering, material engineering, etc.

The specific steps for generating the ice grain model were as follows:

(1) In the PFC software, a two-dimensional plane was established as the Yellow River ice model surface, and its size and location were determined.

(2) Based on the particle size distribution results of ice crystals in the Yellow River ice observation experiment, the particle size of ice grains and their corresponding area contents were determined.

(3) Taking the particle size as the diameter, the corresponding particle flow was generated (as shown in Figure 9), and the coordinates of each center were calculated, output as the seed points, and imported into MATLAB.

(4) A planar space was constructed that conformed to the size of the Yellow River ice in MATLAB; according to the Delaunay algorithm, Delaunay triangles were constructed.

(5) The Delaunay triangles were sorted and the centers of their circumscribed circles were determined.

(6) The centers of the circles were connected in order.

(7) To distinguish different ice crystals, different polygons were given different colors to represent different ice grains (as shown in Figure 10).

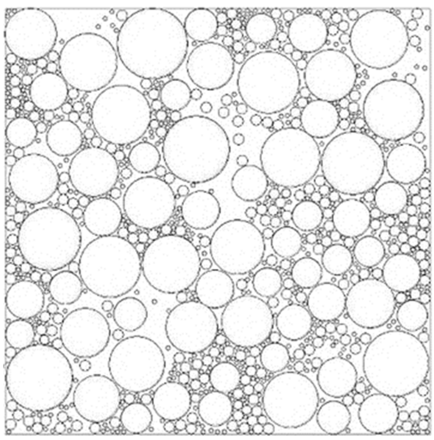

Figure 9. Particle flow corresponding to Voronoi seed points.

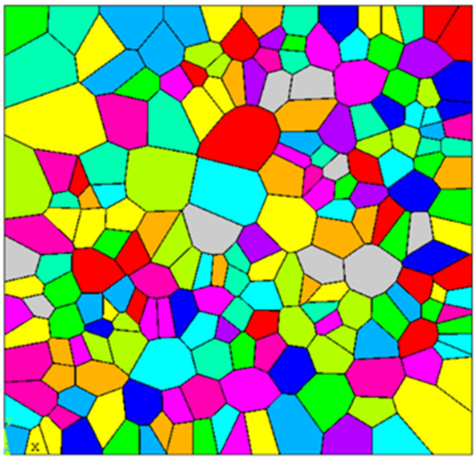

Figure 10. Yellow River ice crystal model.

3.2. Selection of Microscopic Parameters

The microstructural parameters of river ice mainly include the shape, contents, and distribution of its microscopic components. According to the established microscopic river ice model, a random particle flow model was established based on the contents (i.e., proportion of area) of ice grains with different equivalent particle sizes, and the proportions of ice crystals with different sizes were adjusted by the particle flow generated with the PFC. The selected content results of river ice are shown in Figure 11.

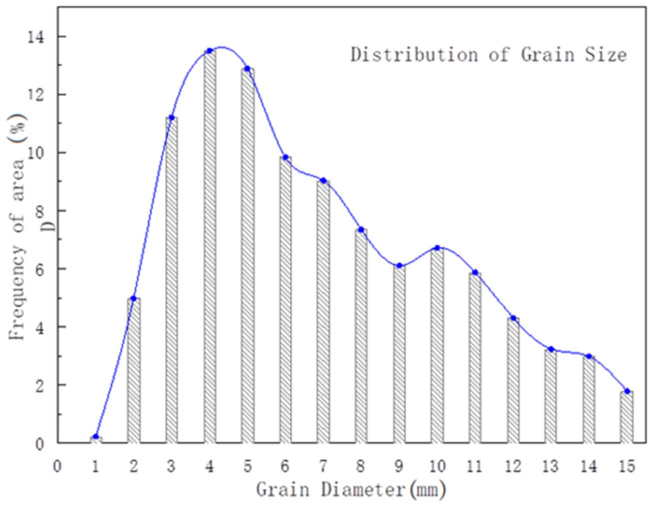

Figure 11. Area proportion of ice grains with different equivalent sizes.

3.3. Simulation Analysis Results

3.3.1. Model Similarity Analysis

The model test size was 300 mm $\times$ 300 mm, with a side length of approximately 40 times the average grain size of Yellow River granular ice. A comparison between the generated river ice sample model and the results of the physical experiment is shown in Figure 12. This comparison between the observed microstructural parameters of Yellow River ice and the microstructural parameters of the model is shown in Table 1, which shows that the established river ice model has a high similarity with the river ice samples. This provides support for the effectiveness and feasibility of the ice model, as well as guarantees for further analyzing the geometric RVE of the river ice microstructure.

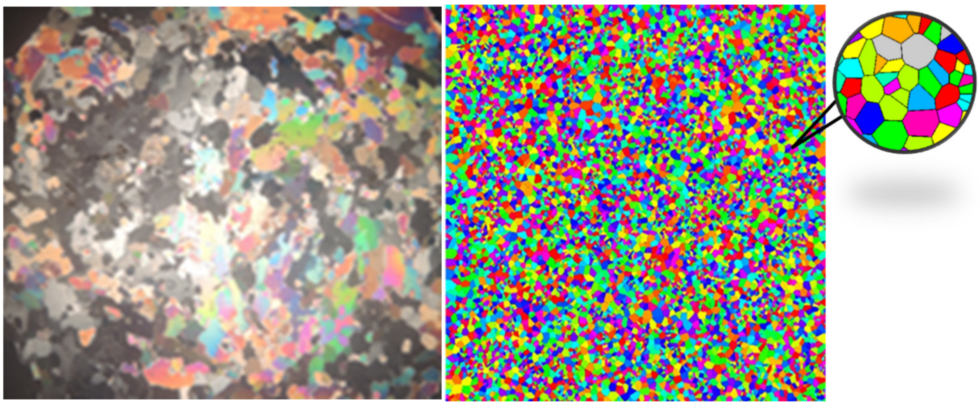

(**a**) (**b**)

Figure 12. Comparison between the simulated ice and the ice samples: (**a**) Typical sample chart of Yellow River ice observation. (**b**) Chart of the Yellow River ice simulation results.

Table 1. Comparison between the test and simulation results of the area contents of different grain sizes.

Grain Size (mm)	Test Results (Area Percentage)	Simulated Results (Area Percentage)
1	0.2	0.052
2	4.98	4.345
3	11.21	14.354
4	13.5	19.001
5	12.88	17.761
6	9.83	13.751
7	9.03	10.941
8	7.34	6.988
9	6.11	5.721
10	6.71	4.15
11	5.87	1.519
12	4.31	1.124
13	3.23	0.127
>14	4.80	0.166
Equivalent grain size	6.903	5.5877

3.3.2. Model Randomness Analysis

To verify the influence of randomness in the numerical ice model, five microscopic numerical sample models of Yellow River ice with the same size were generated. The results of the grain size distribution curves of the generated random samples are shown in Figure 13. There are no significant differences in the area content curves of the river ice grain size. Therefore, this method can establish a microscopic sample model of river ice based on statistical similarity.

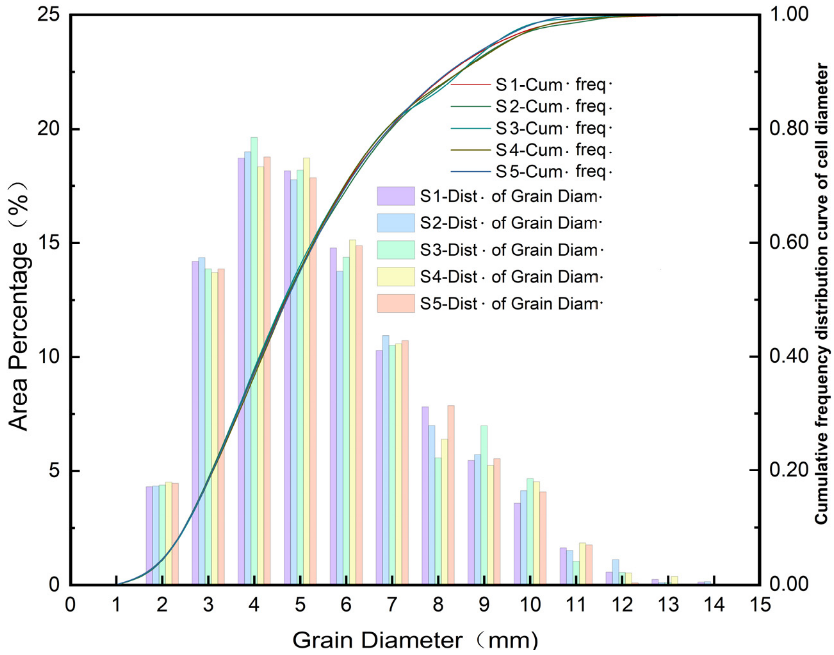

Figure 13. Schematic diagram of the grain size distribution of the Yellow River ice model.

4. Geometric Representative Volume Element of River Ice

At the microscopic level, river ice is a heterogeneous material composed of many ice crystals with different shapes and sizes. The RVE, as a bridging technique connecting the macro- and microscales, plays a key role in the homogenization of random and heterogeneous microstructures.

4.1. Definition of Geometric RVE

According to the definition of RVE by Hill [4] and Starzewski [7], the geometric RVE is very small relative to the macrogeometric scale and is set as ε ($0 < \varepsilon << 1$). The unit contains sufficient microstructure. The material comprises many representative periodic units with periodic physical characteristics, which is shown in Figure 14:

$$F(x + ny) = F(x) \quad (1)$$

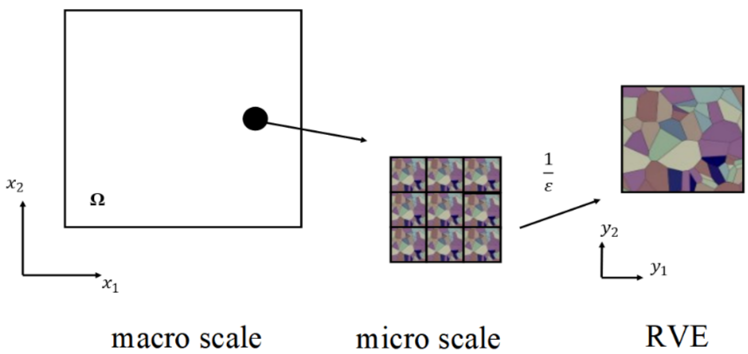

Figure 14. Schematic diagram of the RVE.

Assume that x is the macroscale coordinate and y is the microscale coordinate. On the macroscale, the physical properties of the materials change with the change in x, and the coordinate y can characterize the transformation of the materials from heterogeneity to homogeneity on the microscopic level. The ratio of the true length of the unit vector on the micro-coordinate of the heterogeneous material to the unit vector on the macroscopic coordinate is ε.

$$y = \frac{x}{\varepsilon} \quad (2)$$

On the macroscale, the change in the micro-variables of heterogeneous materials is relatively smooth with the change in x; ε is the relative ratio of the macroscale to the microscale, and $1/\varepsilon$ is a magnification factor for the representative unit to be magnified to the macroscale, which is shown in Figure 14.

To determine the size of the geometric RVE, statistical methods were used to calculate statistics on the changes in river ice microstructure variables with the change in grain size. Different sizes of samples were intercepted from the whole domain, and the RVE value was studied based on the geometric quantity $f_{Li}(xi)$ of each volume element and the geometric quantity $f(x)$ of the whole domain. Here, the subscript Li represents the volume element size. When the geometric quantity in the calculation domain conforms to Formula (3), it can be considered to conform to the RVE size.

$$\frac{f(x) - f_{Li}(xi)}{\sum f(xi)} \leq \varepsilon \quad (3)$$

The method of using the geometric RVE to describe heterogeneous ice in the Yellow River is based on the statistical characteristics of microstructure. A smaller model was used to approximate the characteristics of the overall model. Therefore, after the microscopic samples of the Yellow River ice were generated at random, the overall sample of the Yellow River ice was divided into different subdomains according to the ice grain size. The change effects of grain size, distribution, and geometric shape of different subdomains on the river ice were statistically analyzed, and the geometric RVE of Yellow River ice was studied in combination with numerical analysis. The specific definition of the river ice's geometric RVE is as follows:

(1) The macroscale river ice can be obtained by repeated superposition of the RVE.

(2) The microstructural variables of the RVE tend to be consistent with the values corresponding to the overall material, i.e., there is a volume element that satisfies Formula (3) when it is arbitrarily removed from the overall sample.

(3) The structural variable is not affected by the randomness of the ice sample, such that the variation coefficient of the microstructural variable is less than the allowable error.

An ice sample model that satisfies point (2) as stated above is regarded as a stable scale based on the random error of the ice sample, which is recorded as L_1. The ice sample model satisfying point (3) is regarded as the stability scale based on the overall similarity, which is recorded as L_2. The ice sample model satisfying both points (2) and (3) is regarded as the geometric RVE size of the river ice.

4.2. Determination Method of Geometric RVE

The geometric RVE of the simulated microstructure of river ice was determined by quantifying the real material characteristic variables, such as grain shape and size, crystal orientation, and area content. Then, the microstructure of the river ice was simulated so that the material measurement would be statistically similar to the real experimental microstructure. Finally, the calculation samples of the generated micromodel were intercepted. Therefore, the process of determining the geometric RVE of the river ice was divided into three steps: the selection of statistical variables, the selection of calculation samples, and the determination of the geometric RVE size.

4.2.1. Selection of Statistical Variables

To ensure the rationality of the geometric RVE size, appropriate microstructural variables were selected to study their variation with the river ice size. Because the main load-bearing component of river ice at the microscale is ice crystals, the grain size, distribution, and spatial orientation of ice crystals can be selected as the statistical variables of the geometric RVE of the microstructure. However, according to the observations of river ice's microstructure, granular ice is composed of various homogeneous materials, so the pore size parameters of ice grains—namely, average pore size and relative error—were selected as the statistical variables of the microstructure of the geometric RVE of river ice. The microstructural variables were thus defined as follows:

(1) Average grain size: the weighted average value of the river ice area within each grain size range in the river ice sample, as shown in the following formula:

$$\overline{d} = \frac{\sum_{i=1}^{n} n_i d_i}{\sum n_i} \tag{4}$$

$\overline{d}$—average grain size;
d_i—equivalent grain size of group i;
n_i—percentage grain size in the total area.

(2) Relative error: the percentage of the difference between the average grain size of the calculated ice sample and the average grain size of the overall ice sample, as shown in the following formula:

$$\delta = \frac{d_i - d}{d} \times 100\% \tag{5}$$

δ—relative error;
d_i—equivalent grain size of group i;
d—overall average grain size.

4.2.2. Selection of Calculation Samples

The specific intercept method of the calculated ice sample is shown in Figure 15. In any numerical sample of sufficient size, based on different regional points (i.e., corners, edge center points, center points, and random points), the maximum grain size is regarded as the starting size, and the multiple of the maximum grain size is successively increased. The square size was selected as the calculation sample, from small to large. By selecting appropriate calculation samples, statistical analysis was conducted on the rules of the microstructural variables of the calculation samples to determine the size of the geometric RVE.

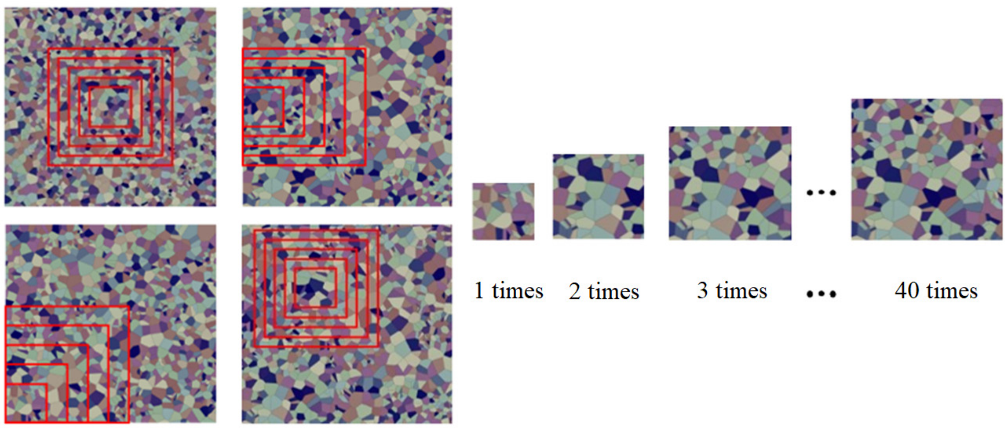

(a) Schematic diagram of calculation sample interception base point (b) Schematic diagram for calculating sample intercept size

Figure 15. Schematic diagram for calculating sample interception.

4.2.3. Process of Determining the Geometric RVE

Based on the definition of the geometric RVE of river ice's microstructure, numerical simulations were used to randomly generate the numerical model of river ice. Based on the results of microscale tests, the distribution of microscale structural variables was extracted, the river ice numerical model was constructed, the overall sample was intercepted based on different regional points, and the distribution of each microscale variable in the calculation sample was statistically analyzed. The specific steps were as follows:

(1) The type and size of ice grains were identified by photographing under the polarizer of the universal stage, and the microstructural variables of the ice were determined by image processing.

(2) The Voronoi algorithm was used to discretize a two-dimensional plane with a suitable size based on the test results to establish a two-dimensional river ice micro-numerical model.

(3) A number of random sample models were generated for each group of parameters, which were taken as the overall samples of river ice. The whole sample was intercepted to obtain the microstructural variables in different calculation sample sizes.

(4) The changes in microstructural variables were statistically analyzed with the change in sample size.

(5) According to Formula (3), the stability scale of the sample was determined based on randomness, which was recorded as L_1.

(6) According to Formula (3), the stability scale was determined based on the overall similarity, which was recorded as L_2.

(7) The larger of L_1 and L_2 was determined as the minimum sample size necessary to meet the uniformity requirements.

4.3. Geometric RVE Results of River Ice

4.3.1. Effect of Entire Ice Sample Size

To analyze the size effect of random samples, random samples of river ice with sizes of 15 times, 25 times, 30 times, 40 times, and 70 times the average grain size were generated. The statistical trend of the microstructural variables in each entire sample was analyzed. The results are shown in Figure 16. E1–E5 are expressed as the change in the average grain size with the overall size when the overall sample size is 15 to 70 times the average grain size. The influence of the entire sample size of river ice on the river ice grain size distribution is shown in Figure 17, where F1–F5 represent the river ice grain size distribution in different samples.

Figures 16 and 17 show that the trends of the microstructural variables of the overall samples with different sizes are inconsistent. The difference in area content between different sizes of river ice is small. When the overall size is less than 300 mm, the average grain size difference of the ice grains is large, up to approximately 4 mm. When the overall size of the river ice is larger than 300 mm, the average grain size tends to be constant at approximately 11 mm. Therefore, when the geometric characteristics of the river ice microstructure are studied, the largest possible overall sample should be selected, and the minimum size should be no less than 30 times the average grain size.

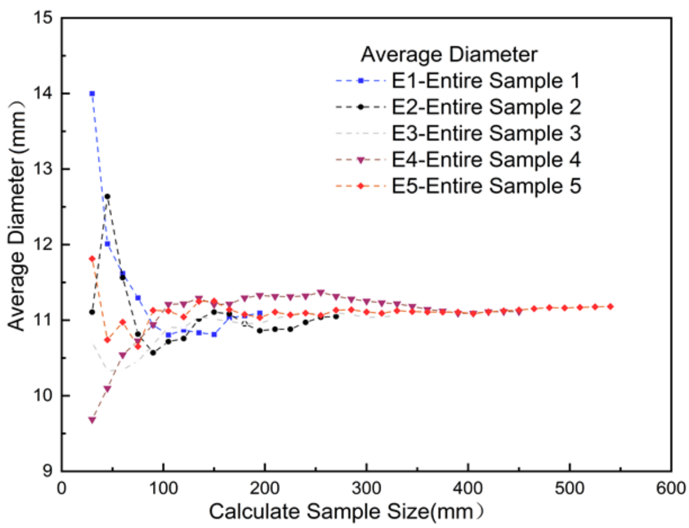

Figure 16. Variation of the average grain size of river ice with calculated sample size.

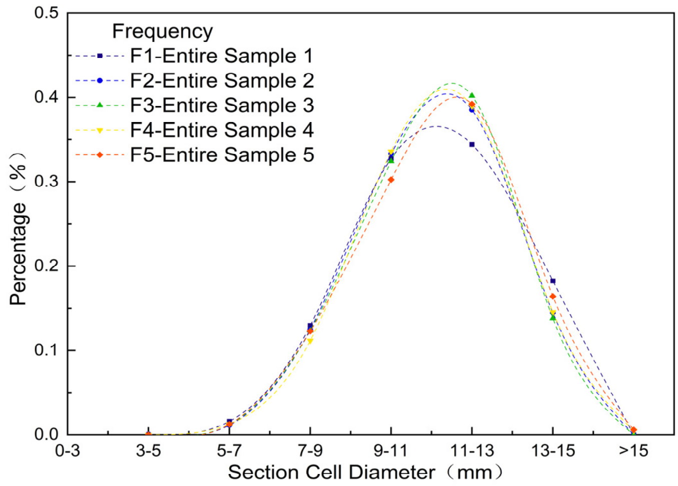

Figure 17. Grain size distribution of river ice in different overall sample sizes.

4.3.2. Randomness Analysis of Ice Samples

The definition of the geometric RVE indicates that the determination of the geometric RVE should account for the randomness of the ice sample and the overall similarity of the RVE. In this section, a random overall sample of river ice with a grain size of less than 15 mm was selected for analysis of random delivery. The overall sample size was 40 times the average grain size; that is, the overall sample size was 300 mm × 300 mm. The calculation samples of different sizes were obtained according to the interception method described in Section 4.2. The geometric RVE size of the Yellow River granular ice was analyzed, and the size of the stability scale was estimated according to an accuracy of 5%.

According to the determination method described in Section 4.2, the change in the microstructural variables in each calculation sample size was statistically analyzed. Calculation samples of the same size were selected from different samples based on different points, from small to large. Figure 18 shows the trend in the coefficient of variation of the average grain size of different samples with the calculated sample size for a given overall sample size.

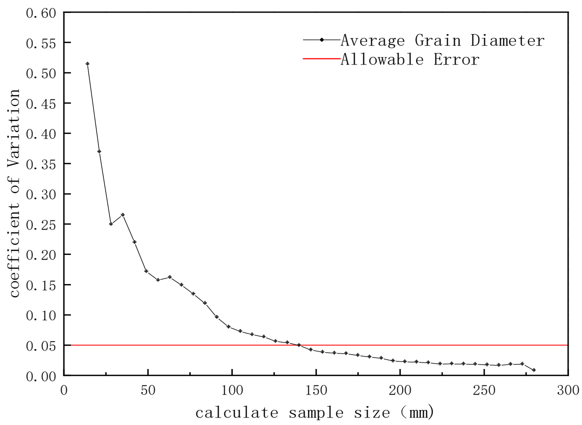

Figure 18. Change in the coefficient of variation of random ice samples with the calculated sample sizes.

The change in the coefficient of variation with the calculated sample sizes shows that the coefficient of variation decreases gradually with the increase in the number of calculation samples. According to the definition of the geometric RVE, and considering the error accuracy of 5% as a standard, the overall similarity stability scale based on the average grain size of river ice is 140 mm (approximately 20 times the average grain size), which is recorded as L_1.

4.3.3. Overall Similarity Analysis

The relative error of the equivalent grain size between different calculation sample sizes and the entire sample was analyzed. Based on the increase in the calculated sample size, the relative error between the calculated samples and the overall sample is shown in Figure 19. Figure 19a–e show the interception results of five samples based on different interception points.

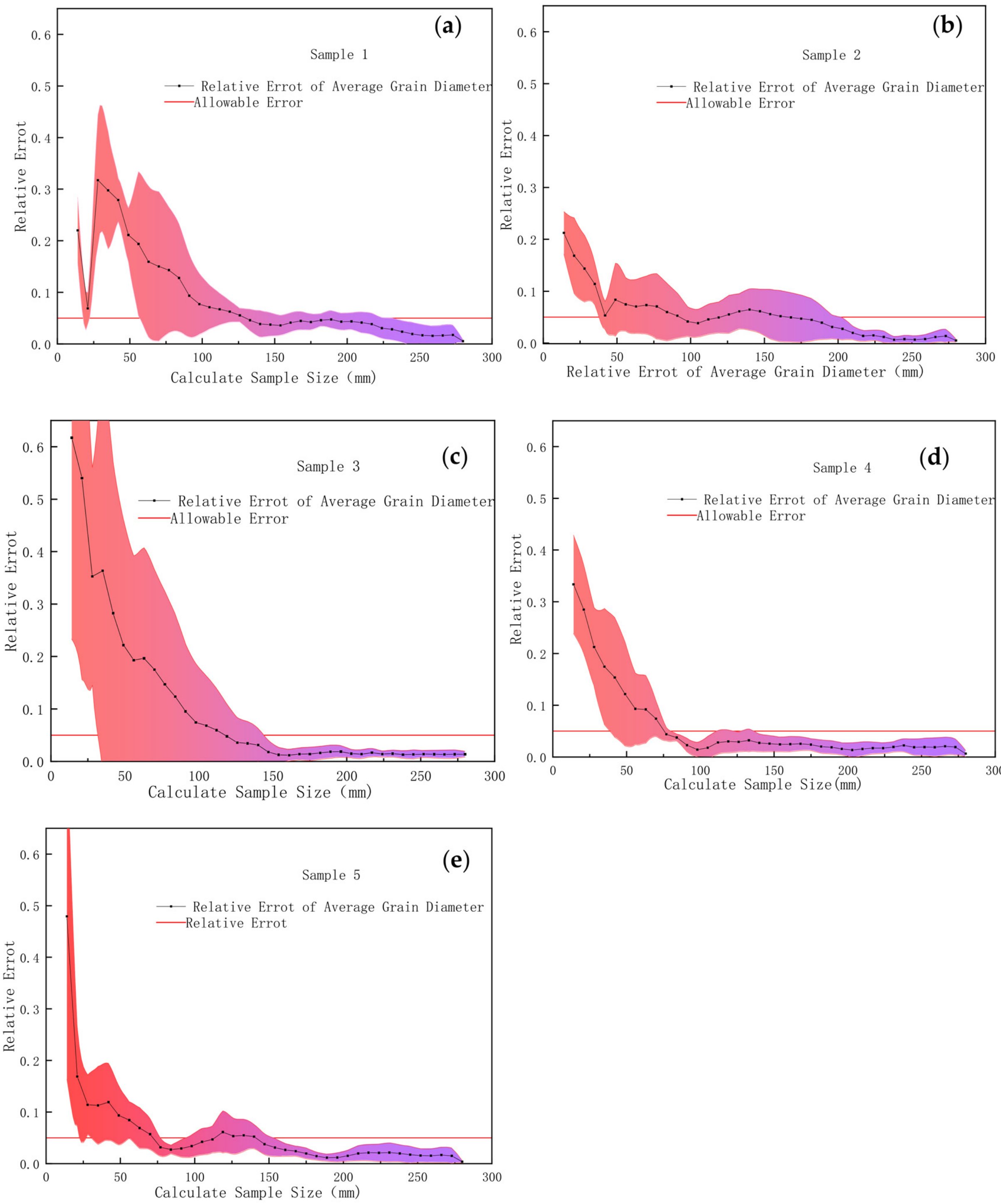

Figure 19. Relative error of the equivalent grain size between different calculation sample sizes and the whole sample size at different base points.

The change in the relative error is different across different simulation samples. When the calculated sample size is small, the relative error of the average grain size is large. However, with the increase in the calculated sample size, the relative error tends to gradually decrease. When the calculated sample sizes of samples 1, 3, and 4 are 133 mm, 119 mm, and 77 mm, respectively, the relative error decreases to below 0.05. With the increase in the calculated sample size, the relative error decreases gradually. However, the average errors of samples 2 and 5 show an upward trend when the sample size is 98 mm and 70 mm, respectively, and gradually decrease after 168 mm and 147 mm, respectively, where they remain below 0.05. According to the definition of the geometric RVE, the larger calculation sample is selected as the overall similarity stability scale, so the overall similarity size L_2 of the Yellow River granular ice is 168 mm (approximately 24 times the average grain size).

The RVE needs to simultaneously meet the requirements of random error stability and overall similarity stability. The microstructural analysis of the 300 mm whole river ice sample shows that the stability scale of randomness is smaller than that of the overall similarity. Therefore, the size of the geometric RVE of the Yellow River granular ice is 24 times the average grain size.

5. Conclusions

Yellow River granular ice was sampled, observed, and analyzed. The features of the Yellow River granular ice's microstructure were summarized. A random sample model of the Yellow River granular ice was established based on statistical similarity. The size of the geometric RVE of the river ice was determined. The heterogeneity of the river ice was studied. Based on these results, a reference for understanding the fracture mechanical properties of the Yellow River ice was provided. At the same time, these results also have important practical significance for promoting the prediction of the river ice break-up period and ice disaster prevention. The main conclusions are as follows:

(1) In the plane perpendicular to the C-axis, ice crystals, bubbles, and sediments are randomly distributed. While there are many ice crystals of granular ice, the equivalent grain size is small and mainly concentrated between 2 mm and 3 mm. With increasing depth, the crystal structure of the cross-section of the granular ice shows little change, and the bubble content in the ice shows a decreasing trend.

(2) After observing the microstructure of river ice, the Voronoi algorithm was used to establish a numerical sampling of river ice according to the distribution characteristics of its microscopic components. The resulting distribution of microscopic components in the numerical sample model was compared with the experimental observation results. The comparison showed that the grain size distribution of the river ice numerical sample model is more consistent with the experimental statistical results.

(3) The concept of the geometric RVE was introduced to describe the microstructure of Yellow River ice. A method for determining the RVE was developed. The average grain size and relative error of ice crystals were selected as the microscopic variables to statistically evaluate the size of the geometric RVE of the microstructure of river ice. Accordingly, the size of the RVE was determined to be approximately 20–24 times the average grain size.

(4) It is feasible to extract the geometric RVE of river ice based on the geometric characteristics of the microstructure of river ice. The results of this research provide a theoretical basis for establishing strength-based RVE and macroscopic models of Yellow River ice.

Author Contributions: Conceptualization, Y.D. and J.W.; methodology, J.Z.; software, J.Z.; data curation, J.Z.; writing—original draft preparation, Y.D. and J.W.; writing—review and editing, P.Z. All authors have read and agreed to the published version of the manuscript.

Funding: This research was supported by the National Natural Science Foundation of China (Grant Nos. 51979024 and 51879116) and the Special Funds for Basic Scientific Research of the Yellow River Institute of Hydraulic Research (HKY-JBYW-2022-08).

Institutional Review Board Statement: Not applicable.

Informed Consent Statement: Not applicable.

Data Availability Statement: Not applicable.

Conflicts of Interest: The authors declare no conflict of interest.

References

1. Guoming, G.; Yu, D.; Zhizong, T. Brief introduction and prospect of recent ice research in the Yellow River. *Yellow River* **2021**, *41*, 77–81.
2. Maolin, S.; Yu, D.; Dong, L. Research progress on the evolution mechanism of ice and its prevention technology in the Yellow River. *Yellow River* **2023**, *45*, 62–67.
3. Yaodan, Z.; Zhijun, L.; Yuanren, X.; Chunjiang, L.; Baosen, Z.; Yu, D. Microstructural characteristics of frazil particles and the physical properties of frazil ice in the Yellow River. *Crystals* **2021**, *11*, 167.
4. Hill, R. Elastic properties of reinforced solids: Some theoretical principles. *J. Mech. Phys. Solid* **1963**, *11*, 357–372. [CrossRef]
5. Hashin, Z. Analysis of composite materials: A survey. *J. Appl. Mech.* **1983**, *50*, 481–505. [CrossRef]
6. Trusov, P.; Keller, I. *The Theory of Constitutive Relations Part I*; Perm State Technical University: Perm, Russia, 1997.
7. Ostoja-Starzewski, M. Microstructural randomness versus representative volume element in thermos-mechanics. *J. Appl. Mech.* **2002**, *69*, 25–35. [CrossRef]
8. Trias, D.; Costa, J.; Turon, A.; Hurtado, J.E. Determination of the critical size of a statistical representative volume element (SRVE) for carbon reinforced polymers. *Acta Mater.* **2006**, *54*, 3471–3484. [CrossRef]
9. Zhan, N. *Study on Multi-Scale Mechanical Behavior of Multistage Porous Bioceramics*; Tianjin University: Tianjin, China, 2011.
10. Forest, S.; Barbe, F.; Cailletaud, G. Cosserat modelling of size effects in the mechanical behaviour of polycrystals and multi-phase materials. *Int. J. Solids Struct.* **2000**, *37*, 7105–7126. [CrossRef]
11. Borges, J.; Pires, L.F.; Cássaro, F.; Roque, W.L.; Heck, R.J.; Rosa, J.A.; Wolf, F.G. X-ray microtomography analysis of representative elementary volume (REV) of soil morphological and geometrical properties. *Soil Tillage Res.* **2018**, *11*, 112–122. [CrossRef]
12. Miska, N.; Balzani, D. Quantification of uncertain macroscopic material properties resulting from variations of microstructure morphology based on statistically similar volume elements: Application to dual phase steel microstructures. *Comput. Mech.* **2019**, *12*, 1621–1637. [CrossRef]
13. Wang, J.; Li, Q.B.; Qing, L.B.; Guan, J.F. Research on geometric representative size of concrete based on statistical characteristics of meso structure. *Eng. Mech.* **2012**, *29*, 1–6. [CrossRef]
14. Wang, J.; Li, X.; Wang, C.X. Quantitative analysis of the representative volume element of polymer grouting materials based on geometric homogenization. *Constr. Build. Mater.* **2021**, *9*, 124223. [CrossRef]
15. Drugan, W.J.; Willis, J.R. A micromechanics-based nonlocal constitutive equation and estimates of representative volume elment size for elastic composites. *J. Mech. Phys. Solids* **1996**, *44*, 497–524. [CrossRef]
16. Kerner, E.H. The elastic and thermo-elastic properties of composite media. *Proc. Phys. Soc. Sect. B* **1956**, *69*, 808–813. [CrossRef]
17. Christensen, R.M.; Lo, K.H. Solutions for effective shear properties in three phase sphere and cylinder models. *J. Mech. Phys. Solids* **1979**, *27*, 315–330. [CrossRef]
18. Herve, E.; Zaoui, A. N-Layered inclusion-based micromechanical modelling. *Int. J. Eng. Sci.* **1993**, *31*, 1–10. [CrossRef]
19. Pensee, V.; He, Q.C. Generalized self-consistent estimation of the apparent isotropic elastic moduli and minimum representative volume element size of heterogeneous media. *Int. J. Solids Struct.* **2007**, *44*, 2225–2243. [CrossRef]
20. Qiaohua, D.; Zhihua, N. Simulation of tensile fracture failure of randomly distributed particle reinforced composites with representative volume element. *J. Mater. Sci. Eng.* **2021**, *39*, 783–790.
21. Yuhong, J.; Na, Y. Calculation method of effective modulus of stone masonry based on RVE elements. *Eng. Mech.* **2022**, *39*, 86–99.
22. Ren, Z.Y.; Zheng, Q.S. A quantitative study of minimum sizes of representative volume elements of cubic polycrystals-numerical experiments. *J. Mech. Phys. Solids* **2002**, *50*, 81–893. [CrossRef]
23. Xu, X.F.; Chen, X.; Shen, L.A. Green-function-based multiscale method for uncertainty quantification of finite body random heterogeneous materials. *Comput. Struct.* **2009**, *87*, 416–1426. [CrossRef]
24. Gitman, I.M.; Gitman, M.B.; Askes, H. Quantification of stochastically stable representative volumes for random heterogeneous materials. *Arch. Appl. Mech.* **2006**, *75*, 9–92. [CrossRef]
25. Gitman, M.I.; Askes, H.; Sluys, L.J. Representative volume: Existence and size determination. *Eng. Fract. Mech.* **2007**, *74*, 2518–2534. [CrossRef]
26. Pelissou, C.; Baccou, J.; Monerie, Y. Determination of the size of the representative volume element for random quasi-brittle composites. *Int. J. Solids Struct.* **2009**, *46*, 842–2855. [CrossRef]
27. Kanit, T.; Forest, S.; Galliet, I.; Mounoury, V.; Jeulin, D. Determination of the size of the representative volume element for random composites: Statistical and numerical approach. *Int. J. Solids Struct.* **2003**, *40*, 647–3679. [CrossRef]
28. Romero, P.; Masad, E. Relationship between the representative volume element and mechanical properties of asphalt concrete properties of asphalt concrete. *J. Mater. Civ. Eng.* **2001**, *13*, 77–88. [CrossRef]
29. Graham, S.; Yang, N. Representative volumes of materials based on microstructural statistics. *Scr. Mater.* **2003**, *48*, 269–274. [CrossRef]

30. Al-Raoush, R.; Papadopoulos, A. Representative elementary volume analysis of porous media using X-ray computed tomography. *Powder Technol.* **2010**, *200*, 69–77. [CrossRef]
31. Yu, D.; Zongkun, L.; Juan, W.; Lukai, X. The microstructure of Yellow River ice in the freezing period. *Crystals* **2019**, *9*, 484.
32. Xinshan, Y.; Xiangyin, M.; Tengfei, J. Object edge detection method based on improved Canny algorithm. *Laser Optoelectron. Prog.* **2023**, *3*, 1–20.
33. Fang, C. Application research of image denoising based on improved median filtering method. *Comput. Inf. Technol.* **2022**, *30*, 18–20.
34. Gao, J.; Revesz, P. Voting prediction using new spatiotemporal interpolation methods. In Proceedings of the 2006 Intenational Conference on Digital Government Research, San Diego, CA, USA, 21–24 May 2006; pp. 293–300.